

**DISCOVERY OF ANDRADITE GARNET AND EVIDENCE FOR HIGH TEMPERATURE HYDROTHERMAL PROCESSES (> 300 °C) IN THE LOWER YAXCOPOIL-1 IMPACT-MELT BRECCIAS.** H. E. Newsom<sup>1</sup>, T. Salge<sup>2</sup>, M. J. Nelson<sup>1</sup>, and M. N. Spilde<sup>1</sup>, MSC03 2050, <sup>1</sup>Univ. of New Mexico, Institute of Meteoritics, Dept. of Earth and Planetary Sciences, Albuquerque, NM 87131 U.S.A. Email: [newsom@unm.edu](mailto:newsom@unm.edu). <sup>2</sup>Bruker AXS Microanalysis GmbH, Schwarzschildstrasse 12, 12489 Berlin, Germany.



**Fig. 1** Image of Unit 5 sample, 861.72 m depth. Al-rich melt clasts are fragmented in a puzzle piece relationship crosscut by a matrix of Mg-rich clays (gray) and calcite (white). The melt clasts are darker near the contact with the matrix (possibly hematite associated with K-metasomatism [12]). The matrix contains smaller fragments of melt clasts surrounded by a fine-grained Mg-rich matrix (darker gray), and calcite (white).

**Introduction:** Hydrothermal processes in large impact craters on Mars may have provided important environments for life and these processes can be studied in analog impact craters such as the 180 km diameter Chicxulub impact [1-3]. The Yaxcopoil-1 drill core in the annular trough of the Chicxulub crater exhibits layered impactites consisting of suevite and impact melt breccias (**Fig. 1**) [4-7]. The use of element mapping techniques at the thin section scale (**Fig. 1**) reveals a complex sequence of mineral growth and dissolution, coupled with the emplacement of matrix material and alteration due to hydrothermal processes.

Evidence for hydrothermal processes in large craters are now well documented, but details of the early high-temperature fluid history are often erased by later lower temperature processes. The recent discovery of zoned andradite garnets (**Figs. 2, 3**) in our thin sections of the lower impact melt breccias (Units 4, 5) from the Yaxcopoil drill core, recognized by T. Salge, provides evidence of the early high temperature fluid system and may record details of the chemistry of the fluids.

**Results:** Microprobe and XRD analyses were conducted at the University of New Mexico, USA, and additional SEM work was conducted by Dr. Tobias Salge in Berlin. The XRD results show the presence of smectite clays in the matrix material, but no evidence for chlorite or other high temperature hydrothermal minerals. However, element mapping reveal the presence of additional evidence for both the high

and low temperature hydrothermal systems. Zoned andradite garnet with Fe-rich rims and Ti-rich cores was identified in the matrix based on morphology and chemical composition [8] (**Table 1**). The garnets are partially dissolved (probably by lower temperature fluids, as seen in the inset to **Fig. 2**). Other common minerals present in the matrix include calcite, halite, and potassium-feldspar grains, which are found in the matrix as isolated grains and in the rims of the Al-rich clasts. Element mapping of the lower melt breccia units at the Yaxcopoil-1 drill core also provide evidence for multiple stages of fracturing of the Al-rich melt clasts, K-metasomatism and injection of Mg-rich material with slightly different chemical signatures.

**Discussion:** The andradite garnet supports the presence of an early high temperature hydrothermal system. Natural occurrences suggest temperatures > 350 °C [9]. The garnet composition also reflects changes in any variable that affect the aqueous speciation of Fe and Al, notably temperature,  $fO_2$ , pH and the salinity of the hydrothermal solution, and changes in the Al/Fe ratio of the pore fluid at the site of crystal

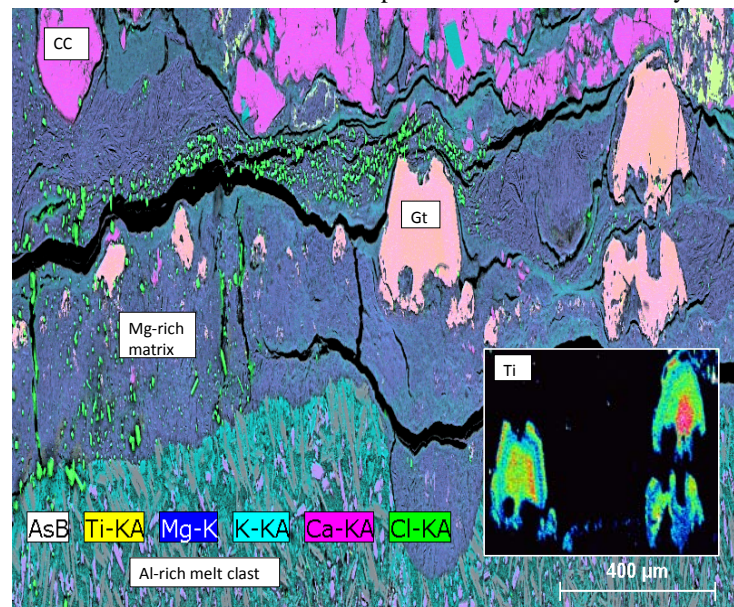


**Fig. 2.** Unit 5 sample, 861.72 m depth. Element map and BSE image of matrix vein (purple). Emplacement of Mg-rich matrix (dark purple) was accompanied by growth of andradite garnet (pink). Partial dissolution of the garnets preceded additional K-metasomatism and deposition of calcite (purple). A final emplacement of Mg-rich material that exhibits more linedated flow texture occurred, with emplacement of halite (green). Inset- Titanium element map showing garnet zoning.

growth [10,11]. The properties of the garnet, especially the negative values of the exchange component  $\text{TiMg}[\text{Fe}^{3+}]_2$ , are consistent with hydrothermal rather than igneous or metamorphic garnets (e.g., Russell et al [11]), reflecting a higher  $f\text{O}_2$  in the fluid. Furthermore, the exchange components suggest, based on the zoning profile, that during formation of the garnets the fluids increased in  $\text{SiO}_2$  activity and increased in  $f\text{O}_2$ , possibly reflecting penetration of surface water.

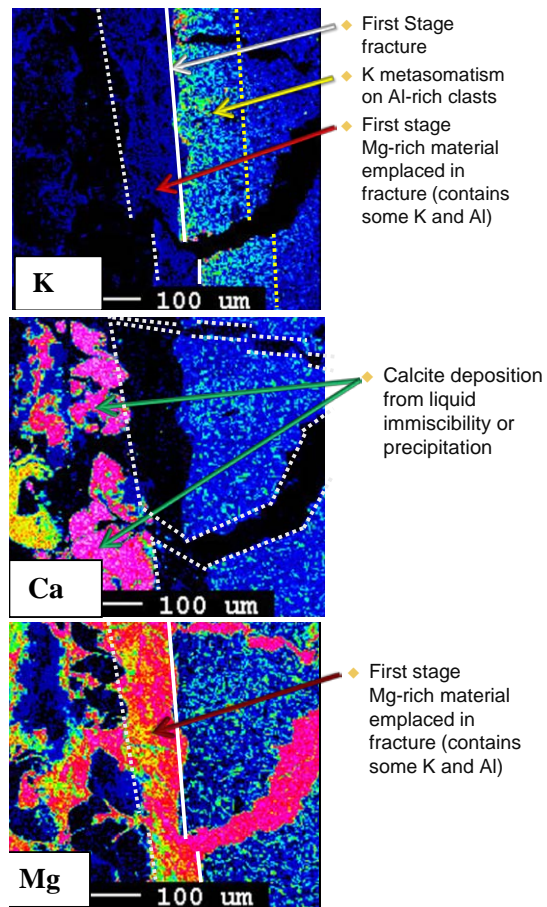


**Fig. 3** Unit 5 sample, 861.72 m depth. The K and Mg maps indicate fracturing of the Al-rich melt clasts with K - enrichment of the edges of the clasts, followed by emplacement of a first stage of Mg-rich material that also contains some Al and K. The Mg and Ca maps show a second stage of fracturing of the Al-rich melt clasts, but these second stage fracture surfaces did not experience a K-metasomatism event. A later stage of injection of Mg-rich material was accompanied by calcite (red) and garnet (yellow - intermediate calcium).

The later evolution of the hydrothermal system apparently led to partial dissolution of the garnets due to lower temperatures. Interestingly, hydrothermal garnets (partially resorbed) were also found in the central uplift of the 36 km diameter Manson structure by McCarville and Crossey [9], although these garnets are almost de-

void of Ti, and may represent formation under lower  $f\text{O}_2$  conditions based on the exchange coefficients.

The nature of the Mg-rich matrix material is still in doubt and must reconcile evidence for multiple stages of emplacement, an extensive hydrothermal alteration episode and a chemical composition that could be consistent with a silic-dolomitic melt.

**Table 1** Preliminary EDS analyses (normalized) to 100% of garnet in the upper right of Fig. 2. The  $\text{TiO}_2$  variation due to zoning is reflected in the center versus rim abundances.

	CaO	FeO	$\text{SiO}_2$	$\text{Al}_2\text{O}_3$	$\text{TiO}_2$	MgO	Total
mean	36.1	22.6	31.7	4.6	4.1	0.8	100
centre	34.7	22.5	31.1	4.6	6.2	1.0	100
rim	35.4	24.9	32.2	4.0	3.0	0.5	100

**Conclusions:** The following sequence of events formed the lower portion of the Yax-1 breccias: (1) Impure dolomite and silicate basement lithologies were melted and ejected during crater formation, (e.g. Stöffler et al [12]), (2) The silicate melt was quenched, brecciated, and enriched in potassium by seawater, or another K-rich fluid during transport or shortly after deposition, and (3) This deposit was later permeated by Mg-rich silicic-dolomitic melt, possibly from melt bodies in the ejecta deposit that were not as well mixed as seen in the upper ejecta material. Alternatively, the early high temperature hydrothermal system could have drastically altered a composition similar to the Al-rich melt clasts. This hydrothermal system at a temperature  $>300^\circ\text{C}$  resulted in early K-metasomatism, formation of zoned andradite garnets, and alteration of the Mg-rich matrix material to smectite clay. The high temperature is consistent with a diopside-hedenbergite, scapolite, sphene and apatite assemblage identified by Zürcher and Kring [7]. Later lower temperature fluids deposited halite and resulted in some late clay deposition [4]. The late stages of the hydrothermal system may have introduced the Li, Be and B measured with the ion probe in the matrix by Newsom et al. [13].

**References:** [1] Newsom H. E. (1980) *Icarus*, 44, 207-216. [2] Newsom H. E. et al. (2001) *Astrobiology*, 1, 71-88. [3] Schwenzer et al. (2010) this meeting submitted. [4] Hecht L., et al. (2004) *MAPS* 39, 1169-1186. [5] Tuchscherer et al. (2004) *MAPS*, 39, 955-978. [6] Ames D.E. et al. (2004) *MAPS*, 39, 1145-1168. [7] Zürcher L., and Kring D. A. (2004) *MAPS*, 39, 1199-1222. [8] Deer et al., (1966) *Rock Forming Minerals*. [9] McCarville P. and Crossey L. J. (1996) *GSA special paper*, 302, 347-376. [10] Jamtveit B. et al. (1995) *Eur. J. Min.*, 7, 1399-1410. [11] Russell J. K. et al. (1999) *Eur. J. Min.*, 11, 919-935. [12] Stöffler D. et al., *MAPS*, 39, 1035-1068. [13] Newsom H. E. et al. (2006) *MAPS*, 41, 1929-1945.

**Acknowledgements:** Samples provided by the Chicxulub Scientific Drilling Project, and funding provided by NASA Planetary Geology and Geophysics grants NNG05GJ42G, and NNH07DA001N (H. Newsom). Discussion with Lutz Hecht and Uwe Reimold were very helpful.